Molecular design strategy for a two-component gel based on a thermally activated delayed fluorescence emitter

*P. Rajamalli, Diego Rota Martir, Eli Zysman-Colman**

Organic Semiconductor Centre, EaStCHEM School of Chemistry, University of St Andrews, St Andrews, Fife, KY16 9ST, UK, Fax: +44-1334 463808; Tel: +44-1334 463826

E-mail: *eli.zysman-colman@st-andrews.ac.uk*

KEYWORDS. TADF emitter, two-component gel, self-assembly, TADF gel, aggregation induced emission.

ABSTRACT Luminescent materials that can spontaneously assemble into highly ordered networks are essential to improve the quality of thin films in stacked device architectures and enhance the performances of solution processed OLEDs. Herein, we report two pyridine-decorated thermally activated delayed fluorescence (TADF) emitters, **3PyCzBP** and **4PyCzBP**. **4PyCzBP** shows robust two component gel formation in the presence of either tartaric acid or succinic acid along with significant emission enhancement. Morphology studies reveal that these gels consist of homogeneous nanofibers assembled in hierarchical supramolecular networks. Transient photoluminescence spectra confirm that the gels emit via a TADF mechanism, making them the first examples of TADF gels. These nanofibers are promising candidates as self-assembled emitting nanofibers in thin films in solution-processed OLEDs.

INTRODUCTION

Recently, there has been an increasing demand to develop low-cost and flexible organic light emitting devices (OLEDs) for flat-panel displays and solid-state lighting sources.[1-3]Although efficient vacuum-deposited small-molecule OLED devices have been developed, solution-processed methods open up the potential for low-cost, flexible, large-area devices. For the most part, efficient solution-processed OLEDs show inferior performance to their vacuum-evaporated analogs.[4-8]This is because solution-processed devices are generally characterised by disordered and non-uniform thin films, which impact negatively on the electronic as well as the optical properties of OLEDs. Therefore, materials that can spontaneously assemble into ordered arrangements that form uniform films are needed to improve the performance of solution-processed OLEDs.[9-11]

In the past few years gelator materials have gained increased attention due to their propensity to form stable three-dimensional (3D) networks through weak intermolecular interactions such as H-bonding, π- π stacking and van der Waals forces.[12-17]Though these materials have been shown to self-assemble into ordered networks that form uniform thin films in stacked device architectures the use of luminescent supramolecular gels in OLEDs is surprisingly still unprecedented. Recently, OLEDs based on metal-free TADF emitters have emerged as a cheaper alternative for phosphorescent organic light emitting diodes (PhOLEDs).[18-21]Similar to phosphorescent organometallic emitters, organic TADF emitters in electroluminescent devices can harvest both singlet and triplet excitons for light emission, achieving up to 100% internal quantum efficiency (IQE). Recently, solution-processed TADF OLEDs have demonstrated comparable performances to their vacuum-deposited counterparts.[22-24]

Herein, we report two novel TADF emitters, **4PyCzBP** and **3PyCzBP**, characterised by a dipyridylcarbazole donor moiety and benzophenone (BP) as the acceptor unit (Fig. 1). The distal pyridines linked to the carbazole engage in hydrogen-bonding with aliphatic diacids such as tartaric acid (TA) and

succinic acid (SA), giving rise to hierarchical supramolecular networks. The fine fibrillar type assembly leads to gelation, which attractively exhibits gelation-enhanced emission (GEE) concomitant with a bathochromic shift in the emission energy. The emission energy and the strength of the gel can both be tuned as a function of the nature of the acid additive. The gel assemblies have been characterized by atomic force microscopy (AFM), transmission electron microscopy (TEM), laser scanning confocal microscopy (LSCM) and powder X-ray diffraction (PXRD). To the best of our knowledge these are the first examples of luminescent gels that emit via a TADF mechanism. Importantly, due to their ordered networks, such gel systems can be attractive emitters for solution-processed OLEDs and other devices.[25-27]

EXPERIMENTAL SECTION

General syntheses of (4-(3,6-di(pyridin-3,4-yl)-9*H*-carbazol-9-yl)phenyl)(phenyl)methanone (3PyCzBP and 4PyCzBP)

The (4-(3,6-dibromo-9H-carbazol-9-yl)phenyl)(phenyl)methanone (0.40 g, 0.79 mmol, 1.0 equiv.), 3-pyridinylboronic acid or 4-pyridinylboronic acid (0.24 g, 1.99 mmol, 2.5 equiv.) and caesium carbonate (1.55 g, 4.75 mmol, 6.0 equiv.) were added to a round-bottomed flask containing 50 mL of a mixture of 1,4-dioxane and distilled water (4:1 v/v). The reaction mixture was degassed by multiple vacuum and N_2 purging cycles, and $Pd(PPh_3)_4$ (0.91 g, 0.079 mmol, 0.1 equiv.) was added to the flask under positive nitrogen pressure. The mixture was refluxed under nitrogen atmosphere for 48 h and then cooled to room temperature. The mixture was poured into distilled water and extracted multiple times with DCM. The organic fractions were combined, washed with a portion of brine and dried over magnesium sulfate. Filtration and evaporation under reduced pressure gave the crude products (1.0 g). The crude products were purified by flash column chromatography (2.5% MeOH/DCM on silica) to give 0.3 g and 0.2 g, respectively for **3PyCzBP** and **4PyCzBP**, of pure compounds as white solids. Characterisation of **3PyCzBP**. **Yield**: 60%. $\boldsymbol{R_f}$ = 0.45 (2.5% MeOH/DCM). **Mp:** 199-200°C. **^{1}H NMR (500 MHz, $CDCl_3$) δ (ppm):** 9.10 – 8.90

(m, 2H), 8.64 (dd, *J* = 4.8, 1.6 Hz, 2H), 8.44 (d, *J* = 1.6 Hz, 2H), 8.15 (d, *J* = 8.4 Hz, 2H), 8.09 – 8.02 (m, 2H), 7.98 – 7.91 (m, 2H), 7.81 (d, *J* = 8.4 Hz, 2H), 7.74 (dd, *J* = 8.6, 1.8 Hz, 2H), 7.70 – 7.65 (m, 3H), 7.59 (t, *J* = 7.6 Hz, 2H), 7.49 (s, 0H), 7.47 – 7.42 (m, 2H). **^{13}C NMR (500 MHz, $CDCl_3$) δ (ppm):** 195.40, 148.33, 147.97, 134.24, 131.91, 129.97, 128.44, 126.23, 125.86, 123.60, 119.08, 110.75 **HR-MS: Calculated:** ($C_{35}H_{24}N_3O$): 502.1914, **Found:** 502.1902. Characterisation of **4PyCzBP**. **Yield**: 40%. R_f = 0.34 (2.5% MeOH/DCM). **Mp**: 200-202°C. **^{1}H NMR (500 MHz, $CDCl_3$) δ (ppm):** 8.74 – 8.70 (dd, 4H), 8.55 – 8.52 (d, *J* = 1.7 Hz, 2H), 8.18 – 8.13 (m, 2H), 7.98 – 7.93 (dd, 2H), 7.82 – 7.77 (m, 4H), 7.72 – 7.7 (m, 4H), 7.68-7.67 (t, 1H), 7.67-7.64 (2H, m), 7.62 – 7.57 (m, 2H). **^{13}C NMR (500 MHz, $CDCl_3$) δ (ppm):** 195.52, 150.25, 148.64, 141.30, 140.77, 137.20, 136.77, 132.88, 132.09, 131.17, 130.09, 128.56, 126.33, 125.84, 124.39, 121.72, 119.23, 110.79. **HR-MS: Calculated:** ($C_{35}H_{24}N_3O$): 502.1914, **Found:** 502.1902.

RESULTS AND DISCUSSION

DFT calculation

The TADF emitters **4PyCzBP** and **3PyCzBP** were synthesized in three steps with overall yields of 19% and 29%, respectively. The detailed synthetic procedures and characterization data are reported in the experimental section and supporting information, respectively. These molecular designs were guided by density functional theory (DFT) calculations, which show spatial separation of the HOMO and LUMO for both emitters. As illustrated in Figure 1, the HOMOs of **3PyCzBP** and **4PyCzBP** are mainly distributed over the dipyridylcarbazolyl group and slightly extended to the bridging phenyl ring. The LUMOs are mostly localized on the benzophenone. The time-dependent DFT (TDDFT) calculated singlet-triplet energy gaps (ΔE_{ST}) are 0.45 eV and 0.41 eV, respectively, for **4PyCzBP** and **3PyCzBP**. The calculated ΔE_{ST} values suggest that these materials may be TADF in nature.[28]

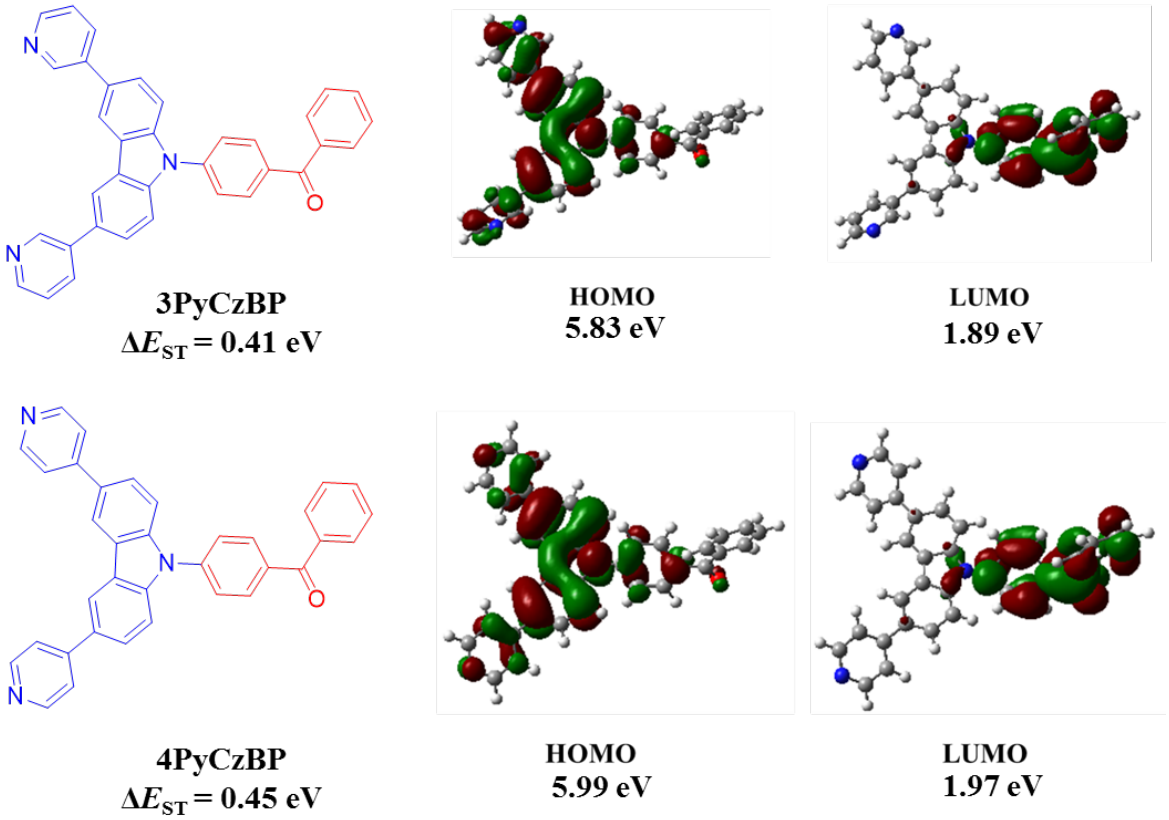

Figure 1. Structure of TADF gelators and corresponding DFT calculated HOMO and LUMO electron density distribution.

Photophysical properties

The DCM solution absorption and emission spectra of the TADF emitters are shown in Figure S9 and S10, respectively and the data are summarized in Tables S3 and S4. Both compounds exhibit a broad absorption band at 356 and 326 nm for **3PyCzBP** and **4PyCzBP**, respectively, assigned to an intramolecular charge transfer (CT) from the carbazole moiety to the BP. In degassed DCM both compounds exhibit broad emission spectra with a λ_{max} at 497 nm and a photoluminescence quantum yield, Φ_{PL} of 56% for **3PyCzBP** and a λ_{max} at 477 nm and a Φ_{PL} of 52% for **4PyCzBP** (Table S2 and Figure S9 and S10). Notably, the Φ_{PL} decreased to 18% and 10%, respectively for **3PyCzBP** and **4PyCzBP** in the presence of O_2 confirming that emission from triplet states, which are readily quenched in the presence of oxygen, contribute to the

radiative decays of these emitters. The emission is blue-shifted when the compounds are dispersed in PMMA films (10 wt%) with λ_{max} at 450 and 449 nm for **3PyCzBP** and **4PyCzBP**, respectively. The Φ_{PL} values under N_2 are 23.4% and 21.0%, which decreased to 19.1% and 17.3% for **3PyCzBP** and **4PyCzBP**, respectively, in the presence of O_2, an indication that triplet states are populated upon photoexcitation in the film.[1]The ΔE_{ST} values in 10 wt% doped PMMA film calculated from peak maximum of the fluorescence and phosphorescence spectra for **3PyCzBP** and **4PyCzBP** are 0.06 eV and 0.07 eV, respectively, while the estimate of ΔE_{ST} based on the emission onset is even smaller at 0.03 eV and 0.05 eV, respectively (Figure S11). Experimentally estimated ΔE_{ST} values (0.03 ~ 0.05 eV) are much lower than the calculated ΔE_{ST} values (0.41 and 0.45 eV); TD-DFT calculations often overestimate ΔE_{ST}.[28-30] The small experimental ΔE_{ST} values indicate that **3PyCzBP** and **4PyCzBP** are TADF materials with efficient thermal up-conversion from T_1 to S_1. The percent contribution of the delayed fluorescence to the overall emission decay for **3PyCzBP** and **4PyCzBP** are 18.3% and 17.7%, respectively.

The transient PL decay characteristics of **3PyCzBP** and **4PyCzBP** 10 wt% doped PMMA under vacuum are shown in Figure S12 and the data summarized in Table S3. Each of the transient decays is triexponential. Prompt fluorescence, τ_p, of 28.0 ns and 33.5 ns, respectively, for **3PyCzBP** and **4PyCzBP** were determined by TCSPC measurements. The delayed fluorescence lifetimes, τ_d, were 0.55 μs, 12.54 μs for **3PyCzBP** and 0.61 μs, 6.32 μs for **4PyCzBP**, an indication of reverse intersystem crossing (RISC) from the triplet to the singlet excited state. Variable temperature transient PL spectra are shown in Figure S13 and S14 and summarised in Table S3. As expected for materials emitting *via* a TADF mechanism, τ_d for both compounds gradually increased with increasing temperature due to the thermally activated RISC. These transient PL decays corroborate the TADF assignment of the emission in doped PMMA films. Electrochemical measurements on **3PyCzBP** and **4PyCzBP** were carried out in MeCN. The cyclic voltammetry (CV) traces are shown in Figure **S15**. The oxidation potentials are for **3PyCzBP** (E_{pa} = 1.69

V vs SCE) and **4PyCzBP** (E_{pa} = 1.71 V vs SCE). The HOMO levels -6.11 and -6.13 eV for **3PyCzBP** and **4PyCzBP**, respectively, were calculated from E_{pa} versus Fc/Fc^+ ($E_{HOMO} = E_{pa} + 4.8$ eV), which are deeper than the HOMO levels of related TADF emitters bearing an unsubstituted carbazole donor and ketone acceptor in D-A-D and D-A systems (ca. -5.7 eV).[28,31] The calculated HOMO values for **3PyCzBP** and **4PyCzBP** are 5.83 and 5.99 eV, respectively, which are shallower than the experimental values. A similar trend is observed for both calculated and experimental HOMO levels, with **4PyCzBP** showing a deeper HOMO value than **3PyCzBP**.

Both compounds are soluble in tetrahydrofuran (THF) and methanol mixture (1:1 v/v) without the formation of aggregates. **3PyCzBP** and **4PyCzBP** are weakly emissive in THF:methanol and THF:methanol:water mixtures (*vide infra*). We initially examined the gelation propensity of the emitters in a 1:1:2 v/v/v THF:MeOH:H_2O mixture, firstly in the absence of any additive. Under these conditions, neither **4PyCzBP** nor **3PyCzBP** showed gel formation. When one equivalent of diacid additive (SA or TA) was added to **3PyCzBP** no gel formation was observed. However, when one equivalent of SA was added to **4PyCzBP**, the colorless solution instantaneously turned to a yellowish green gel with enhanced green emission with λ_{max} at 500 nm (Figure 2, and video in ESI). The critical gel concentration (CGC) for this system was found to be 5 mg/mL. However, as illustrated in Figure 2a, the gel was weak and flowed when the vial was inverted when succinic acid was used as the additive.

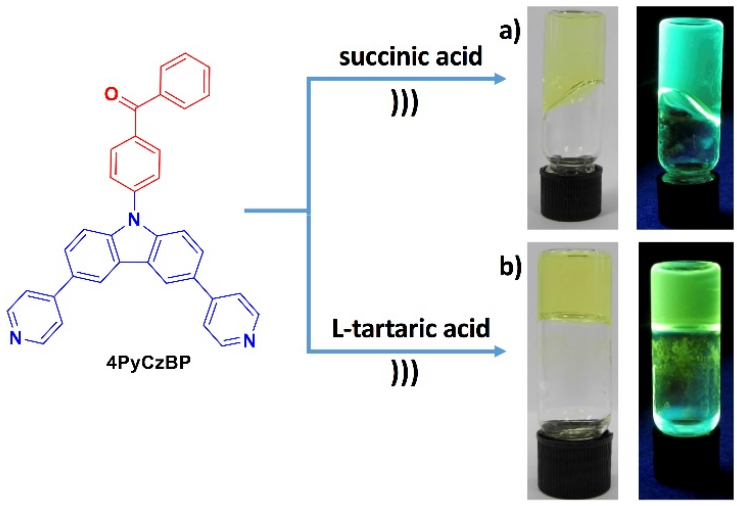

Figure 2. Photograph of gels formed with **4PyCzBP** and a) succinic acid and b) L-Tartaric acid under ambient and UV light.

In order to increase the gelation capacity of **4PyCzBP**, we changed the additive from SA to TA. Due to the higher number of hydrogen bonding sites present in TA a stronger gel formed when one equivalent of TA was added to **4PyCzBP**, with a CGC value reduced from 5 mg/mL to 3 mg/mL (Figure 2b). The emission of the 1:1 **4PyCzBP**:TA gel phase shows broad green emission with λ_{max} at 510 nm. The TA gel shows red-shifted emission (10 nm; 493 cm^{-1}) compared to the SA gel due to stronger packing between the emitter in the presence of TA compare to SA (*vide infra*). This observation is consistent with the observed lower CGC values (3 mg/mL) for the TA gel compared to the SA gel (5 mg/mL); increased viscosity is observed in the TA gel.

The ratio of the TA to **4PyCzBP** was varied from 0.5 to 2 equivalents. In the presence of 0.5 equivalents of TA with **4PyCzBP** a very weak gel formed with an 11-fold emission enhancement (Figure 3a). Both the gelation strength and emission enhancement (60-fold) were increased in the presence of 1 equivalent of TA additive. However, the emission enhancement decreased from 60 to 22 times when the amount of TA was increased further to 2 equivalents. This observed quenching is due to the free TA in the

mixture. This excess of TA destroys the self-assembled gel, which leads to quenching of the emission. Based on the ratio of additive and gelation control experiments a schematic representation for the molecular arrangement in the gel phase is proposed in Figure S16. The formation of gel fibres is presumed to be the result of H-bonding between pyridine and tartaric acid units. UV-vis absorption spectra show that **4PyCzBP** absorbs at 324 nm in THF:MeOH:H_2O (1:1:2 v/v/v). In the presence of one equivalent of SA and TA this absorption band is red-shifted to 389 and 410 nm, respectively, indicating a *J*-type aggregation promoted in the gel phase (Figure S17).[32-33] The TA gel shows a red-shifted (1316 cm^{-1}, 21 nm) absorption spectrum compared to the SA gel, which corroborates a stronger packing of TA gel compared to that of the SA gel. The enhancement in photoluminescence quantum yields for **4PyCzBP**:TA as a function of gelation is also evident in the solid state, Figure 3b. There is a five-fold enhancement upon gelation from 6.0% (neat film) to 36.1% (xerogel gel).

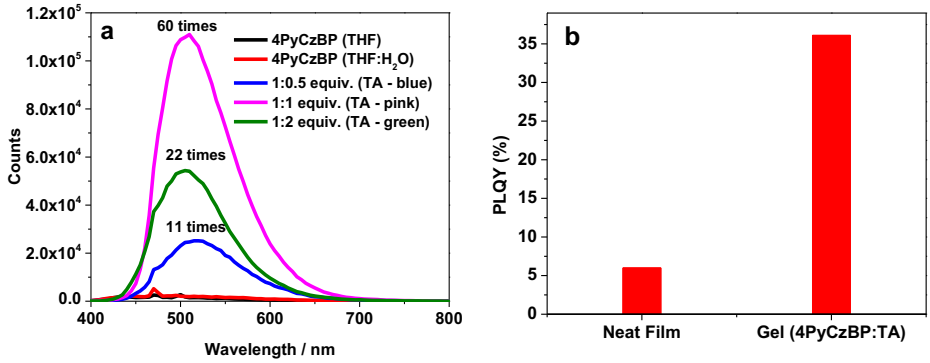

Figure 3. a) PL spectra of **4PyCzBP** with various ratios of TA and b) comparison of PLQY in neat film and gel (**4PyCzBP**:TA).

The presence of H-bonding in the gel has been confirmed by FT-IR where intense peaks at ca. 3265 cm^{-1} indicate H-bonded –OH of the TA. The peak at ca. 1679 cm^{-1} (acid) indicates H-bonded –CO– stretching of TA (Figure S18). The H-bonded –CO– stretch is shifted to lower energy compared to pristine TA (1734 cm^{-1}), suggesting that TA molecules hydrogen bond with each other and with **4PyCzBP** (see

Figure S16). The carbonyl stretching (ketone) of **4PyCzBP** is slightly shifted to lower energy (1648 cm^{-1}) in the gel compared to the pristine emitter (1668 cm^{-1}), which suggests that the ketone is weakly involved in H-bonding.

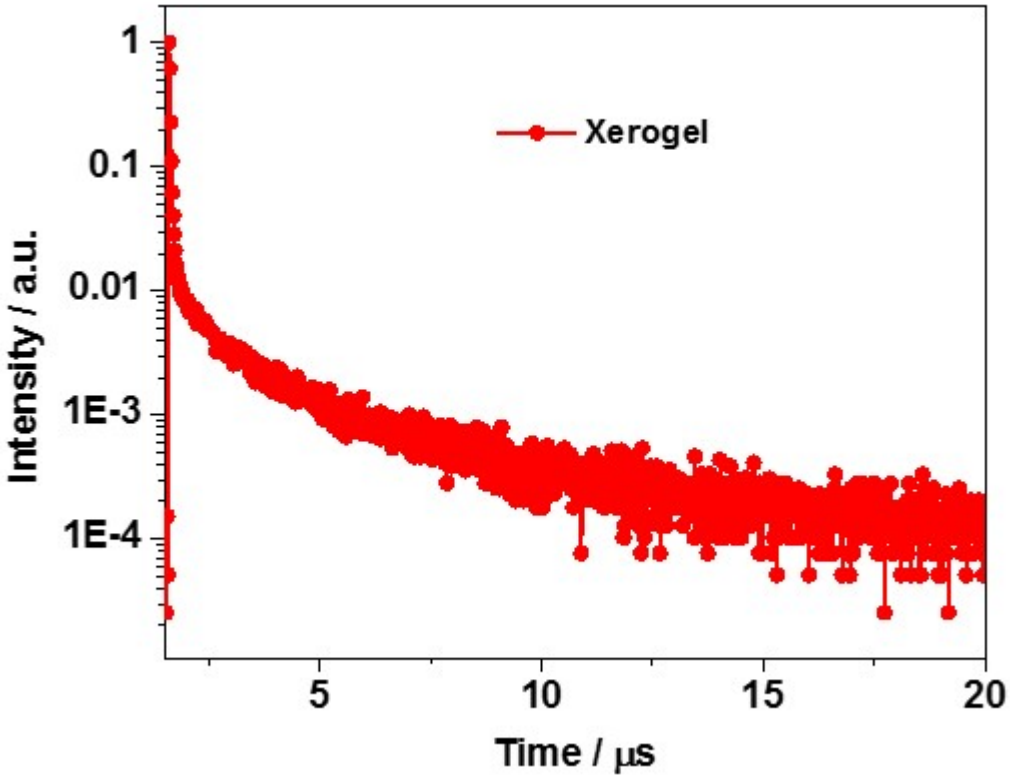

Figure 4. Transient PL spectra of xerogel (1:1 ratio of **4PyCzBP:TA**).

Transient PL measurements were carried out to confirm that the gels remain TADF. Figure 4 shows the characteristic presence of both prompt (τ_p = 20 ns) and delayed (τ_d = 2.3 μs) emission, which supports the TADF nature of the gel. Powder XRD studies (Figure S19) of the dried gel did not reveal the presence of any sharp peaks, which indicates that the gel fibres are amorphous in nature. Atomic force microscopy (AFM) images of the dried gel formed with **4PyCzBP** and SA (xerogel) reveal long and bundled fibres that form highly dense entangled networks (Figure S20). The average diameter of the fibre is in the range of 25-30 nm. The images show fibre heights ranging between 15-20 nm. Intriguingly, the xerogel formed with

4PyCzBP and TA shows long and bundled homogeneous nanofibers. The average diameter of the fibre is 20 nm and the average nanofiber height is 15 nm (Figure 5a). Laser scanning confocal microscopy (LSCM) shows the fluorescing gels (Figure 5b). The confocal microscopic image of **4PyCzBP**:TA gel shows a dense 3D network of greenish fluorescent fibres.

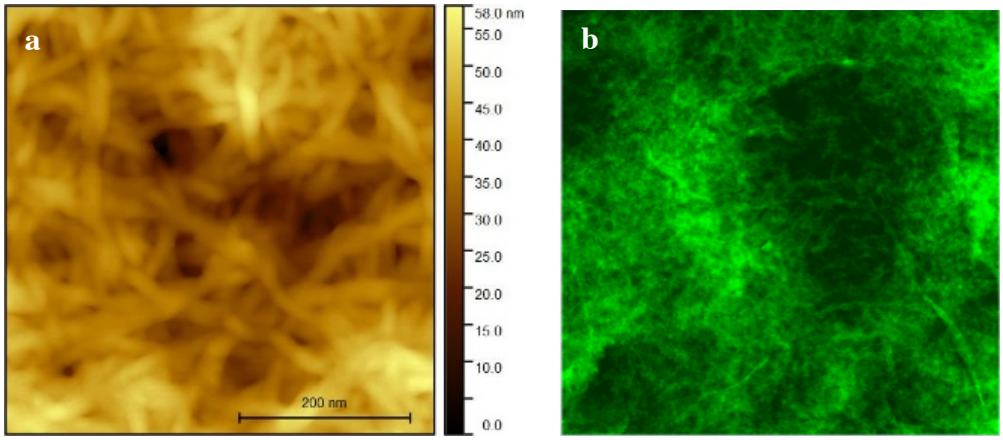

Figure 5. a) AFM image and b) LSCM image of **4PyCzBP**: TA gel.

The morphology was further corroborated by transmission electron microscopy (TEM), as shown in Figure 6. Importantly, the fibre morphology was not damaged by high vacuum, suggesting that these nanofibers are very stable and can be potentially applied as emitting materials in OLEDs.

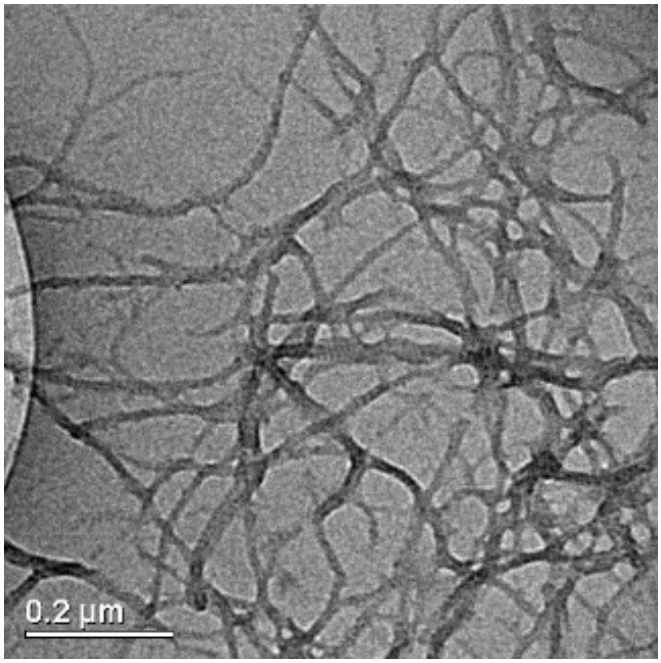

Figure 6. TEM image of 4PyCzBP: TA gel.

CONCLUSIONS

In summary, we synthesized two pyridine-decorated TADF emitters **3PyCzBP** and **4PyCzBP**. Compound **4PyCzBP** shows robust two-component gel formation in the presence of either TA or SA. By contrast, **3PyCzBP** does not form gels. The red-shifted absorption bands of the gels compared with those of THF: MeOH: water (1:1:2 v/v/v) solution were attributed to J-type aggregation in the fibres. Interestingly, these gels show significantly enhanced emission compared to solution. Transient photoluminescence spectra confirm that the xerogels are TADF emitters. Gelation strength and emission energy can both be tuned by varying the additive from succinic acid to tartaric acid. These nanofibers are promising candidates as self-assembled emitting networks in thin films in lighting devices. OLEDs fabrication using these luminescent gels in the emitting layer are currently under progress in our laboratory.

ASSOCIATED CONTENT

Supporting Information

Electronic Supplementary Information (ESI) available: General information, synthesis, characterization data, powder-XRD.

ACKNOWLEDGEMENTS

We thank the Marie Skłodowska-Curie Individual Fellowship (MCIF, no 749557), the Leverhulme Trust (RPG-2016-047) and EPSRC (EP/P010482/1) for financial support. We thank the EPSRC UK National Mass Spectrometry Facility at Swansea University for analytical services.

AUTHOR INFORMATION

Corresponding Author

E-mail: *eli.zysman-colman@st-andrews.ac.uk*

REFERENCES

(1) Rajamalli, P.; Senthilkumar, N.; Gandeepan, P.; Ren-Wu, C.-Z.; Lin, H.-W.; Cheng, C.-H., A Thermally Activated Delayed Blue Fluorescent Emitter with Reversible Externally Tunable Emission. *J. Mater. Chem. C* **2016**, *4*, 900.
(2) Lee, S.-M.; Kwon, J. H.; Kwon, S.; Choi, K. C., A Review of Flexible OLEDs Toward Highly Durable Unusual Displays. *IEEE Transactions on Electron Devices* **2017**, *64*, 1922.
(3) Kwon, J. H.; Choi, S.; Jeon, Y.; Kim, H.; Chang, K. S.; Choi, K. C., Functional Design of Dielectric-Metal-Dielectric-Based Thin-Film Encapsulation with Heat Transfer and Flexibility for Flexible Displays. *ACS Appl Mater Interfaces* **2017**, *9*, 27062.
(4) Reddy, S. S.; Sree, V. G.; Gunasekar, K.; Cho, W.; Gal, Y.-S.; Song, M.; Kang, J.-W.; Jin, S.-H., Highly Efficient Bipolar Deep-Blue Fluorescent Emitters for Solution-Processed Non-Doped Organic Light-Emitting Diodes Based on 9,9-Dimethyl-9,10-dihydroacridine/Phenanthroimadazole Derivatives. *Adv. Optical Mater.* **2016**, *4*, 1236.
(5) Tao, Y.; Guo, X.; Hao, L.; Chen, R.; Li, H.; Chen, Y.; Zhang, X.; Lai, W.; Huang, W., A Solution-Processed Resonance Host for Highly Efficient Electrophosphorescent Devices with Extremely Low Efficiency Roll-off. *Adv Mater* **2015**, *27*, 6939.
(6) Jiang, Z.; Zhong, Z.; Xue, S.; Zhou, Y.; Meng, Y.; Hu, Z.; Ai, N.; Wang, J.; Wang, L.; Peng, J.; Ma, Y.; Pei, J.; Wang, J.; Cao, Y., Highly Efficient, Solution Processed Electrofluorescent Small Molecule White Organic Light-emitting Diodes with a Hybrid Electron Injection Layer. *ACS Appl Mater Interfaces* **2014**, *6*, 8345.

(7) Fu, Q.; Chen, J.; Shi, C.; Ma, D., Solution-processed Small Molecules as Mixed Host for Highly Efficient Blue and White Phosphorescent Organic Light-emitting Diodes. *ACS Appl Mater Interfaces* **2012**, *4*, 6579.
(8) Pu, Y. J.; Chiba, T.; Ideta, K.; Takahashi, S.; Aizawa, N.; Hikichi, T.; Kido, J., Fabrication of Organic Light-emitting Devices Comprising Stacked Light-emitting Units by Solution-based Processes. *Adv Mater* **2015**, *27*, 1327.
(9) Duan, L.; Hou, L.; Lee, T.-W.; Qiao, J.; Zhang, D.; Dong, G.; Wang, L.; Qiu, Y., Solution Processable Small Molecules for Organic Light-emitting Diodes. *J. Mater. Chem.* **2010**, *20*, 6392.
(10) Ohisa, S.; Pu, Y. J.; Yamada, N. L.; Matsuba, G.; Kido, J., Influence of Solution- and Thermal-Annealing Processes on the Sub-nanometer-ordered Organic-organic Interface Structure of Organic Light-emitting Devices. *Nanoscale* **2017**, *9*, 25.
(11) Martín, C.; Kennes, K.; Van der Auweraer, M.; Hofkens, J.; de Miguel, G.; García-Frutos, E. M., Self-Assembling Azaindole Organogel for Organic Light-Emitting Devices (OLEDs). *Adv. Funct. Mater.* **2017,** *27*, 1702176.
(12) Rajamalli, P.; Malakar, P.; Atta, S.; Prasad, E., Metal Induced Gelation from Pyridine Cored Poly(aryl ether) Dendrons with in situ Synthesis and Stabilization of Hybrid Hydrogel Composites. *Chem. Commun.* **2014**, *50*, 11023.
(13) Draper, E. R.; Eden, E. G.; McDonald, T. O.; Adams, D. J., Spatially Resolved Multicomponent Gels. *Nat Chem* **2015**, *7*, 848.
(14) Buerkle, L. E.; Rowan, S. J., Supramolecular Gels Formed From Multi-component Low Molecular Weight Species. *Chem Soc Rev* **2012**, *41*, 6089.
(15) Meazza, L.; Foster, J. A.; Fucke, K.; Metrangolo, P.; Resnati, G.; Steed, J. W., Halogen-bonding-triggered Supramolecular Gel Formation. *Nat Chem* **2013**, *5*, 42.
(16) Weiss, R. G., The past, present, and future of molecular gels. What is the Status of the Field, and Where is it Going? *J Am Chem Soc* **2014**, *136*, 7519.
(17) Rajamalli, P.; Atta, S.; Maity, S.; Prasad, E., Supramolecular Design for Two-component Hydrogels with Intrinsic Emission in the Visible Region. *Chem. Commun.* **2013**, *49*, 1744.
(18) Uoyama, H.; Goushi, K.; Shizu, K.; Nomura, H.; Adachi, C., Highly Efficient Organic Light-emitting Diodes from Delayed Fluorescence. *Nature* **2012**, *492*, 234.
(19) Wong, M. Y.; Zysman-Colman, E., Purely Organic Thermally Activated Delayed Fluorescence Materials for Organic Light-Emitting Diodes. *Adv Mater* **2017**, *29*, 1605444.
(20) Yang, Z.; Mao, Z.; Xie, Z.; Zhang, Y.; Liu, S.; Zhao, J.; Xu, J.; Chi, Z.; Aldred, M. P., Recent Advances in Organic Thermally Activated Delayed Fluorescence Materials. *Chem. Soc. Rev.* **2017**, *46*, 915.
(21) Tao, Y.; Yuan, K.; Chen, T.; Xu, P.; Li, H.; Chen, R.; Zheng, C.; Zhang, L.; Huang, W., Thermally Activated Delayed Fluorescence Materials Towards the Breakthrough of Organoelectronics. *Adv. Mater.* **2014**, *26*, 7931.
(22) Cho, Y. J.; Chin, B. D.; Jeon, S. K.; Lee, J. Y., 20% External Quantum Efficiency in Solution-Processed Blue Thermally Activated Delayed Fluorescent Devices. *Adv. Funct. Mater.* **2015**, *25*, 6786.
(23) Kim, Y. H.; Wolf, C.; Cho, H.; Jeong, S. H.; Lee, T. W., Highly Efficient, Simplified, Solution-Processed Thermally Activated Delayed-Fluorescence Organic Light-Emitting Diodes. *Adv Mater* **2016**, *28*, 734.
(24) Nikolaenko, A. E.; Cass, M.; Bourcet, F.; Mohamad, D.; Roberts, M., Thermally Activated Delayed Fluorescence in Polymers: A New Route toward Highly Efficient Solution Processable OLEDs. *Adv. Mater.* **2015**, *27*, 7236.
(25) Xu, J.; Wang, Y.; Shan, H.; Lin, Y.; Chen, Q.; Roy, V. A.; Xu, Z., Ultrasound-Induced Organogel Formation Followed by Thin Film Fabrication via Simple Doctor Blading Technique for Field-Effect Transistor Applications. *ACS Appl Mater Interfaces* **2016**, *8*, 18991.

(26) Gao, S.; Wang, S.; Ma, J.; Wu, Y.; Fu, X.; Marella, R. K.; Liu, K.; Fang, Y., Salt Tunable Rheology of Thixotropic Supramolecular Organogels and Their Applications for Crystallization of Organic Semiconductors. *Langmuir* **2016**, *32*, 12805.
(27) Bhattacharya, S.; Samanta, S. K., Soft-Nanocomposites of Nanoparticles and Nanocarbons with Supramolecular and Polymer Gels and Their Applications. *Chem Rev* **2016**, *116*, 11967.
(28) Lee, S. Y.; Yasuda, T.; Yang, Y. S.; Zhang, Q.; Adachi, C., Luminous Butterflies: Efficient Exciton Harvesting by Benzophenone Derivatives for Full-color Delayed Fluorescence OLEDs. *Angew Chem Int Ed Engl* **2014**, *53*, 6402.
(29) Rajamalli, P.; Senthilkumar, N.; Huang, P. Y.; Ren-Wu, C. C.; Lin, H. W.; Cheng, C. H., New Molecular Design Concurrently Providing Superior Pure Blue, Thermally Activated Delayed Fluorescence and Optical Out-Coupling Efficiencies. *J Am Chem Soc* **2017**, *139*, 10948.
(30) Chen, X.-K.; Tsuchiya, Y.; Ishikawa, Y.; Zhong, C.; Adachi, C.; Brédas, J.-L., A New Design Strategy for Efficient Thermally Activated Delayed Fluorescence Organic Emitters: From Twisted to Planar Structures. *Adv. Mater.* **2017**, *29*, 1702767.
(31) Rajamalli, P.; Senthilkumar, N.; Gandeepan, P.; Ren-Wu, C. C.; Lin, H. W.; Cheng, C. H., A Method for Reducing the Singlet-Triplet Energy Gaps of TADF Materials for Improving the Blue OLED Efficiency. *ACS Appl Mater Interfaces* **2016**, *8*, 27026.
(32) Wu, H.; Xue, L.; Shi, Y.; Chen, Y.; Li, X., Organogels Based on J- and H-type Aggregates of Amphiphilic Perylenetetracarboxylic Diimides. *Langmuir* **2011**, *27*, 3074.
(33) Li, X. Q.; Zhang, X.; Ghosh, S.; Wurthner, F., Highly Fluorescent Lyotropic Mesophases and Organogels Based on J-aggregates of Core-twisted Perylene Bisimide Dyes. *Chem. Eur. J.* **2008**, *14*, 8074.

Table of Contents (TOC) Graphic: